Structure and vibrational spectra of calcium hydride and deuteride

H. Wu [a,b,*], W. Zhou [a,c], T.J. Udovic [a], J.J. Rush [a], T. Yildirim [a]

[a] *NIST Center for Neutron Research, National Institute of Standards and Technology, 100 Bureau Dr., MS 8562, Gaithersburg, MD 20899-8562, United States*
[b] *Department of Materials Science and Engineering, University of Maryland College Park, MD 20742-2115, Unites States*
[c] *Department of Materials Science and Engineering, University of Pennsylvania, 3231 Walnut Street, Philadelphia, PA 19104-6272, Unites States*

Abstract

We have investigated the structure, energetics, and dynamics of calcium hydride (CaH_2) and calcium deuteride (CaD_2). The crystal structure of CaD_2 (space group *Pnma*) was determined in detail using high-resolution neutron powder diffraction (NPD) data at both 9 and 298 K. The structure is in excellent agreement with the optimized structure derived from first-principles calculations. The phonon calculations based on the optimized structure reproduce well the phonon density of states of CaH_2 (and CaD_2) measured by neutron vibrational spectroscopy (NVS). The combined NPD and NVS results reveal the complete structural and dynamical details for CaH_2 (CaD_2).
© 2006 Elsevier B.V. All rights reserved.

Keywords: Calcium hydride; Calcium deuteride; Neutron powder diffraction; Neutron vibrational spectrum; First principles calculation

Hydrogen is believed to be one of the key alternate clean energy carriers for future transportation and stationary applications, and light-metal hydrides (e.g., LiH, MgH_2, and CaH_2) have long been amongst the most promising prototypes for hydrogen storage because of their innately high hydrogen mass densities. However, at present, no single material fulfills all the requirements for practical hydrogen storage, such as low molar weight, low operation temperature, rapid kinetics, reversibility, and low cost, and there still remain many fundamental scientific and technological challenges before any large-scale utilization of hydrogen becomes a reality. Therefore, it is important to develop a comprehensive database of the fundamental structure and physicochemical properties of these metal-hydride materials, which can aid in the design of improved hydrogen-storage materials in the future. For example, we and others have been investigating how to improve the hydrogen-cycling properties of CaH_2 by adding a destabilizing element such as Si. A basis for such studies is a detailed knowledge of the structure and bonding potentials of CaH_2 and how these properties change with destabilization. While the crystal structure of CaH_2 is known,

the associated local binding potentials of hydrogen have yet to be fully characterized.

The crystal structure of CaH_2 was initially studied by Zintl and Harder [1]. From X-ray data, they identified the *Pnma* symmetry and the metal atomic positions; however, the hydrogen positions were not correctly determined. From a later neutron powder diffraction (NPD) investigation (1962) [2], different hydrogen positions were essentially determined, but the crystallographic study was carried out on data with relatively poor resolution and intensity, and the resultant structure had to rely partly on geometrical considerations. The accuracy of the hydrogen atomic positions was improved by a later NPD study (1977) performed on CaD_2 [3]. Although an early low-resolution neutron vibrational spectroscopy (NVS) study of alkaline-earth hydrides reported a vibrational density of states spectrum for CaH_2, the vibrational bands were poorly resolved and failed to reveal a complete and detailed picture of all phonon modes [4]. In the present study, we reinvestigated the crystal structure of CaD_2 at 9 and 298 K with even greater accuracy using high-resolution NPD. Along with the structure determination, we measured phonon spectra by neutron vibrational spectroscopy (NVS) and performed lattice dynamics calculations using density functional theory, which was used to assign the peaks in the NV spectrum to the corresponding vibrational modes. The characterization and

---

Corresponding author. Tel.: +1 301 975 2387.
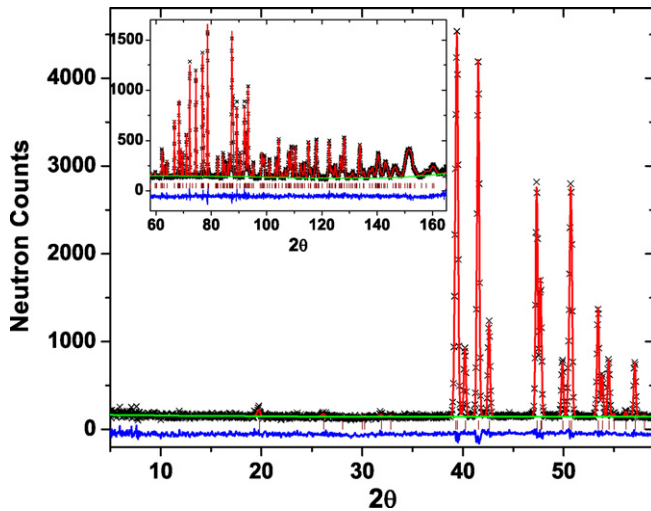*E-mail address:* huiwu@nist.gov (H. Wu).

Fig. 1. Experimental (crosses), calculated (line), and difference profiles for neutron refinement of CaD_2 (298 K). $\lambda = 1.5403(2)$ Å.

calculation of the main features in the NV spectra are consistent with the crystal structure determined from NPD, where phonon contributions come from two distinct hydrogen atomic positions. This study illustrates the utility of combined high-resolution neutron diffraction and spectroscopic techniques for accurately and comprehensively probing both static and dynamic structural information for light-metal hydride materials.

CaH_2 was obtained commercially (99.9%, Aldrich [5]). CaD_2 was prepared by the reaction of Ca metal (Alfa Aesar 99.98% [5]) with D_2 (99.999%) at 773 K. Compositions were determined by pressure–volume–temperature measurements before and after reaction. All neutron scattering measurements were performed at the NIST Center for Neutron Research. Neutron diffraction data for CaD_2 were collected using the BT-1 high-resolution neutron powder diffractometer [6] with the Cu(311) monochromator at $\lambda = 1.5403(2)$ Å and an in-pile collimation of 15 min of arc. Data were collected over the 2θ range of 3–168° with a step size of 0.05°. Rietveld structural refinements were performed using the GSAS package [7]. Neutron vibrational spectra were measured for both CaH_2 and CaD_2 using the filter analyzer neutron spectrometer [8] under conditions

Table 1
Rietveld structure refinement results on CaD_2

	Space group, *Pnma* (62)		Space group, *Pnma* Ref. [3]
	9 K	298 K	
a (Å)	5.92852(5)	5.94753(6)	5.925(1)
b (Å)	3.57774(3)	3.59326(3)	3.581(1)
c (Å)	6.78956(6)	6.80185(7)	6.776(1)
V (Å^3)	144.011(1)	145.362(2)	
R_p (profile)	0.0344	0.0352	
R_{wp} (weighted profile)	0.0402	0.0392	
R_F^2 (Bragg)	0.0322	0.0300	
Reduced χ^2	1.218	0.8999	
Profile function	Pseudo-Voigt (GSAS type 3)		
Background function	Chebyschev polynomial (six coefficients)		

Table 2
Refined structure parameters for CaD_2

	Experimental		Calculated	Ref. [3]
	9 K	298 K	0 K	
Ca1 (4c)				
x	0.2387(1)	0.2397(2)	0.2390	0.2378
z	0.1102(1)	0.1093(1)	0.1096	0.1071
U_{iso} ($\times 100$ Å^2)[a]	0.344(15)	0.904(20)		
D1 (4c)				
x	0.3558(1)	0.3551(1)	0.3546	0.3573
z	0.4276(1)	0.4268(1)	0.4269	0.4269
U_{iso} ($\times 100$ Å^2)[a]	1.293(18)	1.871(23)		
D2 (4c)				
x	0.9750(1)	0.9743(2)	0.9744	0.9737
z	0.6756(1)	0.6759(1)	0.6781	0.6766
U_{iso} ($\times 100$ Å^2)[a]	1.656(19)	2.400(24)		

Ca and D sites were assumed to be fully occupied ($y = 0.25$).

[a] Refined anisotropic thermal displacements ($\times 100$ Å^2) are—9 K Ca: $U_{11} = 0.426(44)$; $U_{22} = 0.268(43)$; $U_{33} = 0.397(45)$; $U_{12} = 0$; $U_{13} = -0.123(32)$; $U_{23} = 0$; D1: $U_{11} = 1.389(37)$; $U_{22} = 1.215(38)$; $U_{33} = 1.224(32)$; $U_{12} = 0$; $U_{13} = 0.161(30)$; $U_{23} = 0$; D2: $U_{11} = 1.687(39)$; $U_{22} = 1.763(39)$; $U_{33} = 1.646(41)$; $U_{12} = 0$; $U_{13} = -0.265(32)$; $U_{23} = 0$; 298 K Ca: $U_{11} = 0.955(57)$; $U_{22} = 0.816(51)$; $U_{33} = 1.015(57)$; $U_{12} = 0$; $U_{13} = -0.115(41)$; $U_{23} = 0$; D1: $U_{11} = 1.919(49)$; $U_{22} = 1.948(50)$; $U_{33} = 1.759(43)$; $U_{12} = 0$; $U_{13} = -0.070(38)$; $U_{23} = 0$; D2: $U_{11} = 2.426(51)$; $U_{22} = 2.400(52)$; $U_{33} = 2.444(55)$; $U_{12} = 0$; $U_{13} = -0.297(42)$; $U_{23} = 0$.

that provided full-width-at-half-maximum energy resolutions of 2–4.5% of the incident energy over the range probed.

The Rietveld structure refinements were performed within the space group *Pnma* (no. 62). The initial atomic positions corresponded to those reported by Andresen et al. [3]. The experimental, fitted, and difference profiles of the neutron diffraction patterns for the final refined structure are shown in Fig. 1. The refined atomic positions yield an excellent fit for the observed

Table 3
Selected atomic distances (Å) in CaD_2

	9 K	298 K
Ca1–D1	2.2639(12)	2.2662(15)
Ca1–D1	2.2477(7)	2.2555(9)
Ca1–D1	2.2477(7)	2.2555(9)
Ca1–D1	2.2841(11)	2.3002(15)
Ca1–D2	2.5055(9)	2.5152(11)
Ca1–D2	2.5055(9)	2.5152(11)
Ca1–D2	2.6307(9)	2.6426(12)
Ca1–D2	2.6307(9)	2.6426(12)
Ca1–D2	2.3936(11)	2.3893(14)
D1–D1	2.6624(12)	2.6809(15)
D1–D1	2.6624(12)	2.6809(15)
D1–D2	2.8162(11)	2.8286(14)
D1–D2	2.6708(8)	2.6777(10)
D1–D2	2.6708(8)	2.6777(10)
D1–D2	2.7457(9)	2.7487(11)
D1–D2	2.7457(9)	2.7487(11)
D1–D2	2.7855(10)	2.7940(13)
D2–D2	2.9952(12)	3.0074(15)
D2–D2	2.9952(12)	3.0074(15)
D2–D2	3.1319(5)	3.1402(6)
D2–D2	3.1319(5)	3.1402(6)

profiles of all the peaks with $R_{wp} = 0.0423$ and $R_p = 0.0362$ at 9 K, and $R_{wp} = 0.0413$ and $R_p = 0.0371$ at 298 K. The final refined crystallographic parameters, atomic positions, thermal parameters, and selected bond distances are summarized in Tables 1–3. The anisotropic thermal displacement parameters of Ca and D atoms are also refined (Table 2) while the difference between each U_{ii} for the corresponding atom is very small. The refined structures at 9 and 298 K indicate that the lattice parameters, bond lengths, and displacement parameters systematically increase with elevated temperature with no significant structural changes. Differences in the present lattice parameters compared to prior results [2,3] may be due to poorer diffractometer resolutions, insufficient 2θ ranges, small errors in neutron wavelengths, or possible different impurity levels and/or CaD_{2-x} stoichiometries in the earlier studies.

Consistent with previous studies [2,3], the crystal structure of CaD_2 provides two different four-fold positions for D atoms: the D1 position is situated within Ca tetrahedra as well as sur-rounded by eight other D atoms; the D2 position is situated within severely distorted Ca octahedra so as to be coordinated with only five Ca neighbors (see Fig. 2). Each D2 position is also surrounded by ten other D atoms. Every Ca atom is coordinated by nine D atoms (four D1 and five D2) with Ca–D bond distances ranging from 2.2477(7) Å to 2.6307(9) Å (at 9 K). The shortest D–D distance is 2.6624(12) Å (at 9 K), which is between two D1 atoms.

Fig. 3 shows the NV spectra of CaH_2 and CaD_2. For H and D atoms vibrating against a rigid or infinitely massive body, the harmonic energy-scaling factor for these two spectra would be $E_H/E_D = \sqrt{m_D/m_H} = \sqrt{2}$. Since the H and D atoms are vibrating instead against relatively light Ca atoms ($m_{Ca} = 40$), the spectra are overlayed assuming a somewhat reduced scaling factor of 1.397, which is the harmonic scaling factor resulting from consideration of the Ca + H and Ca + D reduced masses. A secondary effect that may cause a slightly smaller scaling factor than $\sqrt{2}$ is the fact that the lattice constants for metal deuterides
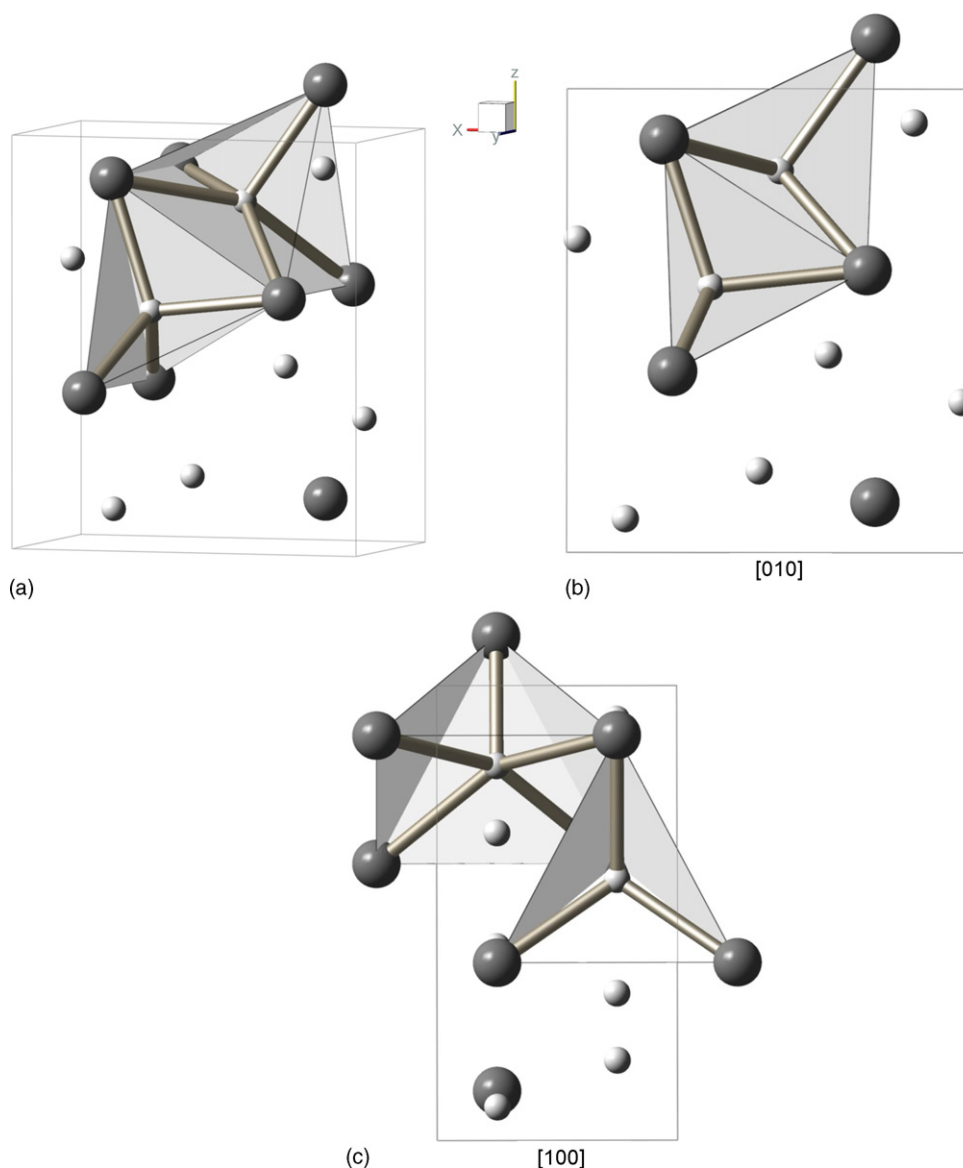

Fig. 2. Refined crystal structure of CaD_2 with two different coordination environments of D atoms. Ca atoms are in grey and D atoms are in white.
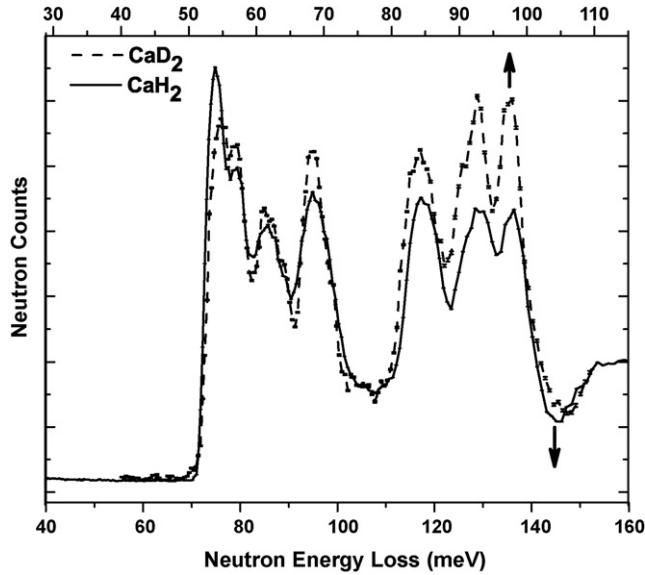
Fig. 3. Measured NV spectra of CaH_2 and CaD_2 at 8 K. The energy scale associated with each spectrum is designated by the arrows. The scaling factor between the two energy axes is 1.397, which is the harmonic value upon consideration of the Ca + H and Ca + D reduced masses.

are typically slightly smaller than their hydride counterparts [9], which will result in slightly different bonding force constants for the two isotopic compounds. Nonetheless, from the observed close overlap, it is clear that the spectra represent essentially the same structure with the same bonding potentials. There are two distinct groups of modes featured in the phonon spectra. To understand the spectra, we performed first-principles dynamics calculations for CaH_2 within the plane-wave implementation of the generalized gradient approximation to density functional theory in the PWscf package [10]. We used a Vanderbilt-type ultrasoft potential with Perdew–Burke–Ernzerhof exchange correlation. A cutoff energy of 408 eV and a $3 \times 6 \times 3$ k-point mesh were found to be enough for the total energy to converge within 0.5 meV/atom. We first optimized the CaH_2 structure. The relaxed atomic positions agreed very well with the experimental values and supported the accuracy of our refined structure (see Table 2). We then performed phonon calculations with the optimized structure using the supercell method with finite difference [11]. A supercell of $2a \times 2b \times 2c$ was used and the full dynamical matrix was obtained from a total of 18 symmetry-independent atomic displacements (0.01 Å). The computed phonon dispersion and phonon density of states are shown in Fig. 4. The primitive cell of CaH_2 contains four formula units (i.e., 12 at.) giving rise to a total of 36 phonon branches. Inspection of the eigenvectors allows the characterization of the modes. The calculated energies at Γ and the dominant contributions from the various atoms are listed in Table 4. The low-energy vibrations (<40 meV) are dominated by Ca displacements. The higher-energy optic vibrations are dominated by H displacements. The phonon modes at Γ are classified as

$$\Gamma (q = 0) = 3[2A_g (R) + A_u + B_{1g} (R) + 2B_{1u} (IR)$$
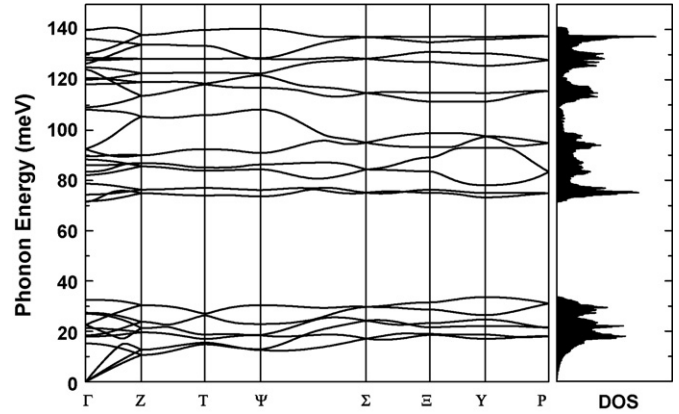$$+ 2B_{2g} (R) + B_{2u} (IR) + B_{3g} (R) + 2B_{3u} (IR)],$$

Fig. 4. Calculated phonon dispersion curves along high-symmetry directions in the Brillouin zone for CaH_2. The phonon density of states is also shown.

where R and IR correspond to Raman- and infrared-active, respectively. The crystal symmetry implies eighteen Raman- and fifteen IR-active modes.

The CaH_2 NV spectrum was computed for a $20 \times 20 \times 20$ q-point grid within the incoherent approximation [11,12] and with instrumental resolution taken into account. As shown in Fig. 5, the agreement between the calculation and the observed

Table 4
Calculated phonon energies E of the optical modes of CaH_2 at the Γ point of the primitive cell

| Species	E (meV)	Dominant character/type
A_u	15.2	Ca/vibration along b
B_{3g}	17.9	Ca/vibration along b
A_g	18.4	Ca/rotation around b
B_{1g}	21.2	Ca/vibration along b
A_g	22.5	Ca/diagonal motion within a–c plane
B_{1u}	22.7	Ca/vibration along a
B_{2g}	27.0	Ca/vibration along c
B_{3u}	27.3	Ca/vibration along c
B_{2g}	32.5	Ca/vibration along a
B_{1u}	71.5	H2/vibration within a–c plane
B_{3u}	71.7	H2/vibration within a–c plane
B_{2u}	74.3	H2/vibration along b
A_u	78.7	H2/vibration along b
B_{1g}	82.2	H2/vibration along b
A_g	83.4	H2/rotation around b
B_{3u}	86.0	H2/rotation around b
B_{3g}	88.3	H2/rotation around b
B_{2g}	89.5	H1, H2/vibration within a–c plane
A_g	92.3	H1, H2/vibration within a–c plane
B_{1u}	92.6	H1, H2/vibration within a–c plane
B_{2g}	108.1	H2/vibration within a–c plane
B_{3u}	109.1	H1/vibration within a–c plane
B_{2g}	118.3	H1, H2/vibration within a–c plane
A_u	120.1	H1/vibration along b
A_g	120.8	H1, H2/vibration within a–c plane
B_{1u}	124.0	H1, H2/vibration within a–c plane
B_{2u}	124.9	H1, H2/vibration along b
A_g	126.5	H1/vibration along c
B_{1g}	127.8	H1/vibration along b
B_{3g}	128.7	H1/vibration along b
B_{1u}	130.6	H1/vibration in a–c plane
B_{2g}	136.3	H1/vibration in a–c plane
B_{3u}	139.8	H1/vibration in a–c plane
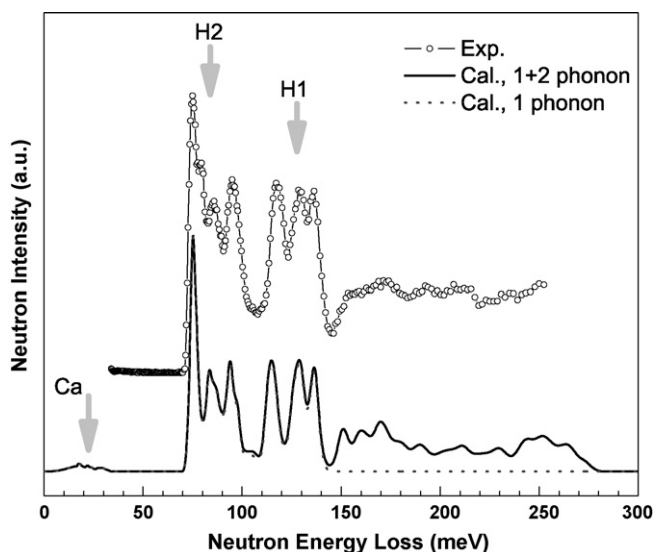
Fig. 5. Calculated NV spectra (bottom) of CaH_2 in comparison with the experimental data. The calculated 1 and 1 + 2 phonon contributions are shown. The low-energy vibrations originate mainly from the Ca atoms. The modes in the higher-energy region (≈ 70–140 meV) are dominated by H character.

spectrum is excellent. Note that the NVS spectrum is dominated by hydrogen displacements. NVS intensities associated with the Ca modes (peaks between 0 and 40 meV) are rather weak and thus were not measured. Below ≈ 140 meV, the spectrum is dominated by one-phonon processes of the H modes. The two-phonon peaks (above ≈ 140 meV) come from the combination of one-phonon processes associated with the peaks in the range of 70–140 meV.

In summary, we have carried out a complete study of the structure, energetics, and vibrational dynamics of calcium hydride (CaH_2) and calcium deuteride (CaD_2) from combined neutron scattering and first-principles calculations. The crystal structure of CaD_2 (space group *Pnma*) has been redetermined with greater accuracy using high-resolution NPD data collected at both 9 and 298 K. The structure is consistent with previous room-temperature diffraction studies and is in excellent agreement with the energy-optimized structure using first-principle calculations. The subsequent phonon calculations based on the optimized structure reproduce very well the measured NVS of CaH_2, which further corroborated the determined structure.

Acknowledgments

References

[1] E. Zintl, A. Harder, Z. Elektrochem. 41 (1935) 33.
[2] J. Bergsma, B.O. Loopstra, Acta Cryst. 15 (1962) 92–93.
[3] A.F. Andresen, A.J. Maeland, D. Slotfeldt-Ellingsen, J. Solid State Chem. 20 (1977) 93–101.
[4] A.J. Maeland, J. Chem. Phys. 52 (8) (1970) 3952–3956.
[5] Certain trade names and company products are identified in order to specify adequately the experimental procedure. In no case does such identification imply recommendation or endorsement by the National Institute of Standards and Technology, nor does it imply that the products are necessarily the best for the purpose.
[6] J.K. Stalick, E. Prince, A. Santoro, I.G. Schroder, J.J. Rush, in: D.A. Neumann, T.P. Russell, B.J. Wuensch (Eds.), Neutron Scattering in Materials Science. II. Mater. Res. Soc. Symp. Proc. No. 376, Materials Research Society, Pittsburgh, PA, 1995, p. 101.
[7] A.C. Larson, R.B. Von Dreele, General Structure Analysis System, Report LAUR 86-748, Los Alamos National Laboratory, NM, 1994.
[8] T.J. Udovic, D.A. Neumann, J. Leão, C.M. Brown, Nucl. Instrum. Meth. A 517 (2004) 189–201.
[9] M. Chiheb, J.N. Daou, P. Vajda, Z. Phys. Chem. 179 (1993) 255.
[10] S. Baroni, A. Dal Corso, S. de Gironcoli, P. Giannozzi, http://www.pwscf.org.
[11] G.L. Squires, Introduction to the Theory of Thermal Neutron Scattering, Dover, New York, 1996.
[12] T. Yildirim, Chem. Phys. 261 (2000) 205–216.